Applied Catalysis B: Environmental 192 (2016) 208–219

Contents lists available at ScienceDirect

Applied Catalysis B: Environmental

journal homepage: www.elsevier.com/locate/apcatb

Solar photocatalytic reduction of Cr(VI) over Fe(III) in the presence of organic sacrificial agents

Belisa A. Marinho [a,b,1], Raquel O. Cristóvão [a,*,1], José M. Loureiro [a], Rui A.R. Boaventura [a], Vítor J.P. Vilar [a,*]

[a] Laboratory of Separation and Reaction Engineering–Laboratory of Catalysis and Materials (LSRE–LCM), Department of Chemical Engineering, Faculty of Engineering, University of Porto, Rua do Dr. Roberto Frias, 4200-465 Porto, Portugal
[b] Capes Foundation, Ministry of Education of Brazil, Brasília – DF 70040-020, Brazil

ARTICLE INFO

Article history:
Received 18 January 2016
Received in revised form 18 March 2016
Accepted 24 March 2016
Available online 29 March 2016

Keywords:
Photocatalytic reduction
Hexavalent chromium
Ferricarboxylate complexes
Organic ligands
Solar photocatalysis

ABSTRACT

Toxic hexavalent chromium reduction to less toxic trivalent chromium was evaluated using a solar driven photocatalytic system, Fe(III)/UV, in the presence of organic sacrificial agents. The photocatalytic reduction experiments were conducted in a lab-scale tubular photoreactor with compound parabolic collectors under simulated solar radiation. The effect of parameters such as iron (1–12 $mg\,L^{-1}$) and citric acid (0.058–3.840 mM) concentrations, pH value (3.0–8.0), temperature (15–40 °C), UVA irradiation source and initial Cr(VI) concentration (1, 10, 20, 40 $mg\,L^{-1}$) on the process efficiency was analyzed, and also the addition of other organic ligands like oxalic acid, maleic acid and EDTA. The presence of citric acid proved to enhance the Cr(VI) reduction by Fe(III)/UV due to the formation of Fe(III)-Citrate complexes, providing a quicker pathway for ferric iron regeneration in the presence of UV–vis light. The organic ligands proved to act also as sacrificial agents of reactive oxygen species formed, avoiding the Cr(III) re-oxidation. The catalytic activity of the organic ligands in the Cr(VI) reduction by Fe(III)/UV followed this order: citric acid > oxalic acid > EDTA > maleic acid. The best Cr(VI) reduction (99% in 15 min) was achieved with citric acid in a Cr(VI):Citric acid molar ratio of 1:3 at pH 5 and 25 °C. Finally, the photocatalytic reduction of Cr(VI) present in a real effluent was achieved after 30 min, demonstrating the potential of the Fe(III)/UVA-vis/citric acid system for the treatment of Cr(VI) containing wastewaters.

1. Introduction

Chromium compounds are widely used in different industrial processes, such as, leather tanning, electroplating, textile dyeing, chemical industry and metallurgy [1]. This leads to the generation of wastewaters containing toxic chromium species at concentrations well above the discharge limits imposed by environmental regulations [2,3]. To face this problem, a strong effort must be done to find new cost-effective technologies for the removal of chromium compounds from those wastewaters, before their discharge into receiving water bodies.

In nature, chromium exists in two major forms, Cr(III) and Cr(VI). The last one has high solubility and toxicity in water [4]. While Cr(III) is only poorly taken up by the human cells, Cr(VI) can easily cross cellular membranes via sulphate transport permeases. Once inside the cell, Cr(VI) is quickly reduced, generating reactive oxygen species, specially hydroxyl radicals, that may cause several DNA mutations and genotoxic effects. The International Agency for Research on Cancer (IARC) has classified Cr(VI) under class 1, i.e. compounds that are known to show sufficient evidence of carcinogenicity in humans [5].

A variety of approaches have been in use for the treatment of chromium containing wastewaters, including ion exchange [6], adsorption [7], chemical or electrochemical reduction [8], membrane filtration [9], precipitation [10], etc.

Fe(II) is one of the dominant Cr(VI) reducing agents. CL:AIRE [11] reported a real case of groundwater contamination with Cr(VI) where the application *in situ* of an acidified solution of ferrous sulphate heptahydrate led to 99.95% of Cr(VI) removal by a reductive precipitation mechanism. In this process, the Cr(VI) was reduced to Cr(III) (Eq. (1)), and further precipitated as $Cr(OH)_3$ (Eq. (2)), at neutral pH [12].

$$Cr^{6+} + 3Fe^{2+} \rightarrow Cr^{3+} + 3Fe^{3+} \quad (1)$$

* Corresponding authors.
E-mail addresses: raquel.cristovao@fe.up.pt (R.O. Cristóvão), vilar@fe.up.pt (V.J.P. Vilar).
[1] These authors contributed equally to this work.

http://dx.doi.org/10.1016/j.apcatb.2016.03.061
0926-3373/

$$Cr^{3+} + 3OH^- \rightarrow Cr(OH)_{3(s)} \quad (2)$$

The main drawback of this treatment system for Cr(VI) containing industrial wastewaters is the high amount of iron required and the generation of high amounts of sludge, that need additional treatment. Fe(II) is generally considered to reduce Cr(VI) quickly at acidic conditions, but rate constants at near-neutral pH values have not been reported. Since the early 19th century, it has been reported the Fe(III) reduction to Fe(II) with the generation of some reactive species by photochemical dissociation of hydroxylated Fe(III) complexes [13]. In this way, the regenerated Fe(II) may reduce the Cr(VI), and the generated reactive oxygen species can oxidize, at the same time, the organic compounds present in aqueous solution. Actually, inorganic pollutants usually coexist in the natural environment with organic matter or organic pollutants and it is possible to apply decontamination simultaneously [14]. Therefore, the Cr(VI) photocatalytic reduction in the presence of Fe(III)–water and Fe(III)-organic complexes under UV–vis light seems to be a good option, reducing the amount of chemicals needed to treat diluted Cr(VI) solutions. Liu et al. [14] studied the use of Fe(III)–OH complexes to promote the reduction of Cr(VI) and, simultaneously, the oxidation of bisphenol A (BPA) in a photocatalytic system. The results showed a synergic effect in the ternary system: both Cr(VI) photocatalytic reduction and BPA degradation rates were higher in the Fe(III)/Cr(VI)/BPA system.

It is known that the photoreduction of ferric to ferrous ions depends on two main parameters: pH and Fe(III)–organic ligand complexes/metal ratio values [13]. In this work, the photoreduction treatment of hexavalent chromium in aqueous solution and present in a real galvanic wastewater was investigated using different Fe(III)-organic ligands complexes (e.g. Fe(III)-citrate complexes, Fe(III)-oxalate, Fe(III)-EDTA, etc.). The effect of parameters such as pH, Cr(VI) initial concentration, Fe(III)-organic ligands complexes dosage, temperature and irradiance source was also assessed in order to optimize the photoreduction treatment.

So, this work aims to go a step forward in the perception of the key step to maximize the photocatalytic reduction of Cr(VI) in the presence of Fe(III) and organic acids.

2. Material and methods

2.1. Chemicals

Cr(VI) and Cr(III) aqueous solutions were prepared from $K_2Cr_2O_7$ (Merck, purity 99.9%) and $Cr(NO_3)_3{\cdot}9H_2O$ (Carlo Erba) salts. Cr(VI) concentration was determined by colorimetry using 1,5-diphenylcarbazide (Merck, purity 98%). Iron(III) chloride hexahydrate (Merck), oxalic acid dihydrate (VWR Prolabo, purity 98%), citric acid monohydrate (VWR Prolabo, purity 98%), maleic acid (Fluka, purity 99%) and disodium EDTA (M&B, purity 98.5%) were used in the photocatalytic experiments. Sulphuric acid (Pronalab, 96%, 1.84 g/cm^3) and sodium hydroxide (Merck) were used for pH adjustment. All samples were filtered through 0.45 μm cellulose acetate membranes (Sartorius) before analysis.

2.2. Analytical determinations

Total chromium concentration was determined by atomic absorption spectrometry (AAS, GBC 932 Plus) with a nitrous oxide-acetylene flame, a spectral slit width of 0.2 nm and a working current/wavelength of 6.0 mA/357.9 nm, giving a detection limit of 0.08 mg L^{-1}. The hexavalent chromium concentration was measured by molecular absorption spectrophotometry with a detection limit of 2.05 μg L^{-1}. The procedure followed is based on the formation of a pink complex of Cr (VI) with 1,5-diphenylcarbazide in acid solution, which absorbs at 540 nm. Dissolved iron concentration was determined by colorimetry with 1,10-phenantroline according to ISO 6332 [15].

2.3. Actinometric experiments

The photonic fluxes entering the reaction systems were determined by potassium ferrioxalate method [16], 2-nitrobenzaldehyde (2-NB) adapting the method proposed by Willett and Hites [17] and hydrogen peroxide actinometry method [18]. The experimental procedures of all these methods for each irradiation source studied (UVA–vis lamp (xenon arc lamp 1700 W), installed inside the solar radiation simulator (ATLAS, model SUNTEST XLS); UVA lamp (Philips fluorescent blacklight blue lamp, 6 W energy power, model TL 6W/08); UVA–vis lamp (Luxram® UVA–vis lamp, 6 W energy power); UVC lamp (Philips UVC low pressure mercury lamp, 6 W energy power, model TUV G6T5); natural sunlight) are described in Supplementary Material.

For all actinometries, the concentrations-time (CT) plot was fitted to zero-order kinetics and Eq. (3) enabled to calculate the photonic flux, F_0 (Einstein s^{-1}):

$$F_0 = \frac{d[CT]}{dt} \times \left(\frac{1}{\varphi}\right) \times V \quad (3)$$

where $d[CT]/dt$ is the zero-order kinetic constant (mol L^{-1} s^{-1}), ϕ is the quantum yield of: i) ferrioxalate at the lamp wavelength (1.25 at 250–500 nm) ii) 2-NB at the lamp wavelength (0.41 at 280–400 nm); iii) hydrogen peroxide at the lamp wavelength (1.25 at 253.7 nm); and V is the solution volume (L).

Afterwards, in all actinometries, the photonic flux was converted to J s^{-1} (*pf*) from:

$$pf = F_0 \times E \times N_A \quad (4)$$

where E is the energy (J) calculated from Plank's equation for: i) λ_x = 407 nm of both UVA–vis lamps; ii) λ_{max} = 360 nm of the UVA lamp; iii) λ_{max} = 253.7 nm of the UVC lamp and N_A is Avogadro's number (6.022×10^{23} mol^{-1}).

Note that the calculation of the photonic flux depends on the fraction of light absorbed by the actinometer. However, for the high actinometer's concentration and the path length used, this parameter can be omitted since it is very close to unity.

2.4. Experimental units

The experiments were carried out in three different experimental units: i) a lab-scale sunlight simulator photoreactor; ii) a lab-scale lamp photoreactor and iii) a CPC solar pilot plant.

2.4.1. Lab-scale photoreactor

2.4.1.1. Apparatus. The lab-scale photoreactor experimental set-up was already published by Soares et al. [19]. A detailed description can be seen in Supplementary material, as well as the respective schematic representation (Fig. S1).

2.4.1.2. Experimental procedure. The recirculation glass vessel of the lab-scale prototype was filled with 1.5 L of Cr(VI) solution (1, 10, 20, 40 mg L^{-1}), which was pumped to the CPC unit and homogenized by recirculation in the closed system during 15 min in the darkness. Afterwards, citric acid was added (0.058–3.840 mM), pH was adjusted in the range 3.0–8.0 and controlled with sulphuric acid/sodium hydroxide, and ferric chloride (1–12 mg L^{-1}) was added. Samples were taken after each addition before turning on the SUNTEST. The temperature set-point of the refrigerated thermostatic bath was adjusted to keep the intended solution temperature (15–40 °C). Then the SUNTEST was turned on and the irradiance was set at 300 or 500 W m^{-2} which is equivalent to photonic fluxes (*pf*) of 1.38 and 1.80 J s^{-1}, respectively, determined

Table 1
Characteristics of UVA, UVA–vis and UVC lamps, natural sunlight and SUNTEST 300 and 500 W_{uv} m^{-2} irradiation sources.

Light source	Average UV intensity (280–400 nm) (W_{UV} m^{-2})[a]	Photonic flux (300–410 nm)[b] ($J s^{-1}$)	Photonic flux (250–450 nm)[c] ($J s^{-1}$)	Photonic flux (250–500 nm)[d] ($J s^{-1}$)
UVA lamp	30.0[e]	0.65 ± 0.04[e]	–	0.85
UVA–vis lamp	0.3[e]	–	–	0.23 ± 0.02[e]
UVC lamp	0[e]	–	0.72 ± 0.04[e]	–
Natural sunlight	25.0 – 31.1	3.57[f]	–	10.24[f]
SUNTEST 300	27.1	0.34[f]	–	1.38[f]
SUNTEST 500	43.9	0.44[f]	–	1.80[f]

[a] Measured by a global UV radiometer (Kipp & Zonen B.V., model CUV5).
[b] Determined by 2-NB concentration actinometry.
[c] Determined by H_2O_2 actinometry.
[d] Determined by ferrioxalate actinometry using $[Fe(C_2O_4)_3]^{3-}$ ion prepared *in situ*.
[e] Determined by Moreira et al. [21,35].
[f] Irradiated area/solution volume (cm^2 L^{-1}): Natural sunlight = 300; SUNTEST 300 and 500 = 170.

by ferrioxalate actinometry and of 0.34 and 0.44 J s^{-1}, respectively, determined by 2-NB actinometry The accumulated energy ($Q_{UV,n}$, kJ L^{-1}) received on any surface in the same position, per unit of water volume inside the reactor, in the time interval Δt_n, is calculated by Eq. (5):

$$Q_{UV,n} = Q_{UV,n-1} + pf\frac{\Delta t_n}{1000 \times V_t}; \Delta t_n = t_n - t_{n-1} \quad (5)$$

where t_n is the time corresponding to n-water sample (s) and V_t is the total reactor volume (L).

2.4.2. Lab-scale lamp photoreactor

The experiments regarding the use of UVC, UVA and UVA–vis radiation were carried out in a lab-scale lamp photoreactor (Fig. S2), consisting of: i) a gear pump (Ismatec, model BVP-Z); ii) a cylindrical glass vessel equipped with a cooling jacket coupled to a refrigerated thermostatic bath (Lab. Companion, model RW-0525G); iii) a magnetic stirrer (Velp Scientifica, model ARE); iv) pH and temperature meter (VWR symphony—SB90M5); v) a borosilicate tube (Schott-Duran type 3.3, Germany, cut-off at 280 nm, internal diameter 70 mm, length 200 mm and thickness 1.8 mm) associated to a concentric inner quartz tube with 22 mm external diameter where the lamp is housed. The characteristics of the lamps are given in Table 1. Two polypropylene caps with four equidistant inlets and outlets ensured a better distribution of the feed stream throughout the photoreactor. The borosilicate tube was located in the focus of two stainless steel reflectors (double CPC), each one consisting of two truncated parabolas and exhibiting a total horizontal dimension of 19.5 cm × 21.0 cm, one at the bottom and another at the top, allowing illumination along the total tubular reactor perimeter and minimizing radiation losses. The accumulated energy ($Q_{UV,n}$, kJ L^{-1}) received inside the reactor is calculated by Eq. (5). The photonic fluxes (*pf*) were: 0.65 and 0.85 J s^{-1} for the UVA lamp determined by 2-NB and ferrioxalate actinometers, respectively; 0.23 J s^{-1} for the UVA–vis lamp determined by ferrioxalate actinometry; 0.72 J s^{-1} for the UVC lamp determined by H_2O_2 actinometry. The adopted experimental procedure was equal to the one used in the lab-scale photoreactor.

2.4.3. Solar CPC pilot plant

2.4.3.1. Apparatus. Solar driven photocatalytic experiments were carried out in a CPC pilot plant (Fig. S3) installed at the roof of the Chemical Engineering Department of the Faculty of Engineering, University of Porto (FEUP), Portugal, that was already used by Pereira et al. [20]. A detailed description can be seen in Supplementary material.

2.4.3.2. Experimental procedure. At the beginning of the experiment, a weighted amount of Cr(VI) was added to 15 L of demineralized water, previously added to the recirculation tank, which was pumped to the CPC unit and homogenized by recirculation in the closed system during 15 min in the darkness. The experimental procedure, considering the chemicals addition and the sampling, was equal to the one described for the lab-scale system. After all reagents addition, in the same order as described in Section 2.4.1.2, the CPCs were uncovered and samples were collected at predetermined times (t). The photoreduction reaction was conducted using a Cr(VI) concentration of 10 mg L^{-1}, initial pH = 5.0, $[Fe^{3+}]$ = 2.0 mg L^{-1}, Cr(VI):citric acid molar ratio of 1:3.

The solar UV irradiance was measured with a global UV radiometer (Kipp & Zonen B.V., model CUV5), placed in the pilot plant with the same inclination of the reactor, which provides data in terms of incident W_{UV} m^{-2}, measured in the wavelength range from 280 to 400 nm. The photonic fluxes (*pf*) were 3.57 and 10.24 J s^{-1} determined by 2-NB and ferrioxalate actinometers, respectively, considering a total CPCs area of 0.455 m^2 and an average solar UV power during the experiment of 29 W_{UV}/m^2. The accumulated energy ($Q_{UV,n}$, kJ L^{-1}) received on any surface in the same position, per unit of water volume inside the reactor, in the time interval Δt_n, is calculated by Eq. (5).

2.5. Wastewater characterization

The real wastewater sample was collected in an electroplating industrial company and used without previous treatment. Table 2 presents the main characteristics of the Cr(VI) containing wastewater from the galvanization process. The photoreduction reaction of the real wastewater was conducted in the lab-scale photoreactor (SUNTEST at 500 W m^{-2}) using $[Fe^{3+}]$ = 8.0 mg L^{-1} and a Cr(VI):citric acid molar ratio of 1:3.

3. Results and discussion

3.1. Effect of citric acid concentration on the photocatalytic reduction of Cr(VI) by Fe(III)/UVA–vis/citric acid system

The toxic hexavalent chromium (10 mg L^{-1}) reduction to less toxic trivalent chromium by Fe(III)/UVA–vis/citric acid photocatalytic system was firstly evaluated in the lab-scale photoreactor (SUNTEST at 500 W m^{-2}) at pH 3.0 and 25 °C. In this experiment it was used a Fe(III) concentration corresponding to the discharge limit for total iron (2 mg L^{-1}) imposed by Portuguese regulations (Decree-Law No. 236/98) and equal citric acid molar concentration. It is well known that Fe(III) and citrate bind in a stoichiometry of 1:1, generating mononuclear complexes [21]. However, after 60 min of reaction it was only achieved a Cr(VI) reduction of 21%. The reaction was also evaluated in the absence of citric acid leading to a removal of only 11%. According to Moreira et al. [21], $FeOH^{2+}$ is the most pho-

toactive Fe(III)-hydroxy complex, with a molar fraction of 22.5% at the abovementioned conditions (Fig. S4a). The photoreduction of this species results in the generation of both Fe(II) and hydroxyl radicals (Eq. (6)), leading to chromium reduction by ferrous ions (Eq. (1)), but also to its reoxidation by the hydroxyl radicals formed (Eq. (7)).

$$FeOH^{2+} + h\nu \rightarrow Fe^{2+} + HO^{\bullet} \quad (6)$$

$$Cr^{5+}/Cr^{4+}/Cr^{3+} + HO^{\bullet} \rightarrow Cr^{6+}/Cr^{5+}/Cr^{4+} + OH^{-} \quad (7)$$

The reaction with citric acid in the absence of Fe(III), with and without UVA–vis irradiation, results in approximately 12% of Cr(VI) reduction. In the absence of Fe(III), but without irradiation, the observed Cr(VI) reduction may due to the reducing nature of the scavenger agent used; in other hand, with radiation, the Cr(VI) photoreduction is accompanied by citric acid simultaneous oxidation via photoinduced electron transfer (PET), which plays the role of electron donor [22]. Wittbrodt and Palmer [23] reported also a slow Cr(VI) reduction only in the presence of dissolved organic compounds. In turn, Li et al. [24] did not observe a noticeable Cr(VI) concentration decrease using citric acid for 22 h. Therefore, despite the presence of dissolved organic matter, the Cr(VI) contamination in subsurface waters, lakes and wetlands can spread over large areas before its substantial reduction.

A Cr(VI) reduction of approximately 13% was achieved in the presence of both citric acid and Fe(III) without UVA–vis irradiation. The enhancement of Cr(VI) reduction to 21% with UVA–vis irradiation is attributed to the role of ferricitrate complexes in Fe(II)/Fe(III) photochemical cycle that occurs only in irradiated systems. In fact, ferric ions form stable and strong complexes with citric acid that i) have much higher quantum yields than ferric iron-water complexes; ii) can use a higher fraction of the solar radiation spectrum, up to 580 nm; iii) are photodecarboxylated under visible radiation; iv) provide a quicker pathway for Fe(III) regeneration accelerating thereby the process [25]. The Fe(III) complexes species present in the aqueous solution are function of pH. The speciation diagram obtained by the chemical equilibrium modelling system MINEQL+ for an iron concentration of 2 mg L^{-1} and equal molar ratio of citric acid at 25 °C (Fig. S4b of Supplementary material) shows the molar fraction of Fe(III) species in the Fe(III)-cit aqueous solution. At pH 3, [Fe(Cit)] and $[FeOH(Cit)]^{-}$ are the predominant species (23.5 and 32.6%, respectively). According to literature [26,27], these species are reported to photochemically induce weak oxidizing species formation, such as $O_2^{\bullet -}$ and H_2O_2. Beyond that, in the ternary system, citric acid acts also as sacrificial agent of reactive oxygen species, avoiding the Cr(III) re-oxidation, while the simultaneous reduction of Cr(VI) to Cr(III) is attributed to Fe(II). Due to its dual function, a higher citric acid amount is probably necessary to promote the total Cr(VI) reduction. The reaction runs in cycle until all Cr(VI) is reduced or all citric acid is consumed.

This way, a new set of photoreduction experiments were performed using 10 mg L^{-1} of Cr(VI), pH 3.0, 25 °C, 2 mg L^{-1} of ferric ions and varying the citric acid concentration through different Cr(VI):citric acid molar ratios (1:0.5; 1:1; 1:1.5; 1:2; 1:3; 1:4; 1:20). Fig. 1 shows the effect of citrate concentration on Cr(VI) photoreduction as a function of reaction time.

Several authors reported the Cr(VI) reduction by organic acids in the presence of Fe(III) as a pseudo-first order kinetic model [24,28]. However, in this work it was found that the Cr(VI) photoreduction followed a zero order reaction kinetics. The kinetic constant, k, was evaluated according to $C = C_0 - k \times t$, where C represents the Cr(VI) concentration at time t and C_0 is the initial Cr(VI) concentration. Table 3 presents the kinetic parameters for all the photoreduction experiments.

From the results presented in Table 3 it is possible to observe that the photoreduction rate is almost constant until a Cr(VI):citric

Table 2
Characteristics of the galvanic wastewater.

Parameters	Units	Values
pH	Sörensen Scale	6.7
Temperature	°C	20
Conductivity	μS cm^{-1}	608
Turbidity	NTU	2.7
Total suspended solids (TSS)	mg TSS L^{-1}	< 0.1
Dissolved organic carbon (DOC)	mg C L^{-1}	5.9
Inorganic carbon (IC)	mg C L^{-1}	1.5
Total Chromium	mg Cr L^{-1}	38
Hexavalent Chromium	mg Cr(VI) L^{-1}	36
Trivalent Chromium	mg Cr(III) L^{-1}	2.0
Sodium	mg Na L^{-1}	89
Magnesium	mg Mg L^{-1}	9.4
Potassium	mg K L^{-1}	66
Zinc	mg Zn L^{-1}	10
Calcium	mg Ca L^{-1}	66
Lithium	mg Li L^{-1}	0.02
Fluoride	mg F L^{-1}	0.51
Chloride	mg Cl L^{-1}	28
Nitrite	mg NO_2 L^{-1}	2.0
Nitrate	mg NO_3 L^{-1}	23

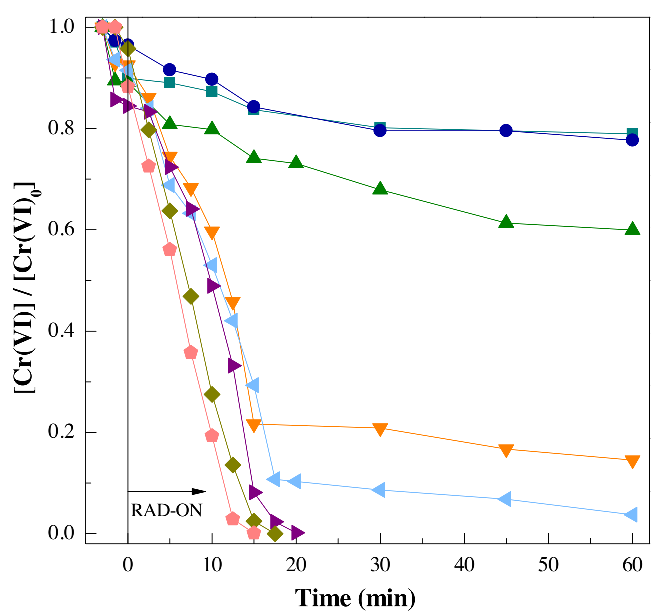

Fig. 1. Influence of citric acid concentration on Cr(VI) photocatalytic reduction ([Cr] = 10 mg L^{-1}) by Fe(III)/UVA–vis/citric acid system in the lab-scale phot-reactor (SUNTEST at 500 W m^{-2}). [Fe(III)] = 2 mg L^{-1}, pH = 3, T = 25 °C. Cr(VI)/citric acid molar ratio—Fe(III)/citric acid molar ratio = (■) 1:0.2–1:1, (●) 1:0.5–1:2.7, (▲) 1:1–1:5.3, (▼) 1:1.5–1:8.0, (◀) 1:2–1:10.7, (▶) 1:3–1:16.0, (◆) 1:4–1:21.3, (⬟) 1:20–1:106.7.

acid molar ratio of 1:4, increasing only for a molar ratio of 1:20. However, it can be seen from Fig. 1 that the ratio of 1:3 is enough to reduce the Cr(VI), reaching the complete reduction in less than 15 min. This behavior was observed in other systems, for example in the Cr(VI) reduction with salicylic acid [29] and in the presence of TiO_2 nanoparticles [30]. This result shows that a Cr(VI):citric acid molar ratio of 1:3 is enough to maintain the citric acid concentration in a value to ensure that the Fe(III)-citrate complex formation cycle occurs throughout the entire reaction. For lower ratios, the citric acid concentration seems to be not enough and the Cr(VI) reduction stops when all citric acid is consumed, not forming the Fe(III)-citrate complex again.

At a given pH, the Fe(III) to citrate concentration ratio determines the Fe(III)-citrate complexes species distribution in the aqueous solution, corresponding to different photoactivities [31]. As inferred from Fig. S5 of the Supplementary material, at pH

Table 3
Zero order kinetic constants for photocatalytic Cr(VI) reduction by Fe(III)/UV–vis/citric acid system along with the corresponding coefficient of determination (R^2) and residual variance (S^2r).

Experiment	[Cr(VI)] ($mg\,L^{-1}$)	[Fe(III)] ($mg\,L^{-1}$)	Cr(VI):citric acid ratio	pH	T (°C)	k ($mg\,L^{-1}\,min^{-1}$)	R^2	$S^2{}_r$ ($mg\,L^{-1}$)^2
Influence of Cr(VI):citric acid ratio								
1.1	10	2	1:1[a]	3.0	25.0	0.050 ± 0.007	0.876	0.045
1.2	10	2	1:0.5	3.0	25.0	0.048 ± 0.007	0.923	0.025
1.3	10	2	1:1	3.0	25.0	0.055 ± 0.007	0.920	0.063
1.4	10	2	1:1.5	3.0	25.0	0.32 ± 0.02	0.984	0.039
1.5	10	2	1:2	3.0	25.0	0.47 ± 0.02	0.993	0.043
1.6	10	2	1:3	3.0	25.0	0.49 ± 0.01	0.996	0.029
1.7	10	2	1:4	3.0	25.0	0.50 ± 0.01	0.995	0.034
1.8	10	2	1:20	3.0	25.0	0.59 ± 0.01	0.998	0.012
Influence of iron concentration								
2.1	10	1	1:3	3.0	25.0	0.30 ± 0.01	0.991	0.024
2.2	10	2	1:3	3.0	25.0	0.49 ± 0.02	0.996	0.029
2.3	10	4	1:3	3.0	25.0	0.88 ± 0.04	0.993	0.085
2.4	10	8	1:3	3.0	25.0	1.49 ± 0.04	0.999	0.018
2.5	10	10	1:3	3.0	25.0	1.75 ± 0.02	0.999	0.003
2.6	10	12	1:3	3.0	25.0	1.65 ± 0.05	0.998	0.026
Influence of pH								
3.1	10	2	1:3	3.0	25.0	0.49 ± 0.02	0.996	0.029
3.2	10	2	1:3	3.5	25.0	0.52 ± 0.02	0.994	0.050
3.3	10	2	1:3	4.0	25.0	0.52 ± 0.02	0.995	0.040
3.4	10	2	1:3	4.5	25.0	0.53 ± 0.02	0.994	0.053
3.5	10	2	1:3	5.0	25.0	0.62 ± 0.02	0.995	0.052
3.6	10	2	1:3	6.0	25.0	0.17 ± 0.02	0.958	0.052
3.7	10	2	1:3	7.0	25.0	0.077 ± 0.007	0.965	0.009
3.8	10	2	1:3	8.0	25.0	0.06 ± 0.01	0.903	0.015
Influence of temperature								
4.1	10	2	1:3	5.0	15.0	0.15 ± 0.02	0.931	0.393
4.2	10	2	1:3	5.0	17.5	0.210 ± 0.007	0.990	0.061
4.3	10	2	1:3	5.0	20.0	0.47 ± 0.04	0.963	0.254
4.4	10	2	1:3	5.0	25.0	0.62 ± 0.02	0.995	0.052
4.5	10	2	1:3	5.0	30.0	0.57 ± 0.02	0.990	0.092
4.6	10	2	1:3	5.0	35.0	0.56 ± 0.02	0.993	0.072
4.7	10	2	1:3	5.0	40.0	0.57 ± 0.03	0.980	0.189
Influence of initial Cr(VI) concentration (Cr(VI):citric acid:[Fe(III)])								
5.1	1	2	1:30	5.0	25.0	0.210 ± 0.006	0.995	0.001
5.2	10	2	1:3	5.0	25.0	0.62 ± 0.02	0.995	0.052
5.3	20	2	1:1.5	5.0	25.0	0.236 ± 0.006	0.995	0.058
5.4	40	2	1:0.75	5.0	25.0	0.22 ± 0.01	0.982	0.181
5.5	1	2	1:3	5.0	25.0	0.083 ± 0.007	0.970	0.003
5.6	20	2	1:3	5.0	25.0	0.40 ± 0.02	0.985	0.613
5.7	40	2	1:3	5.0	25.0	0.181 ± 0.005	0.991	0.230
5.8	1	0.2	1:3	5.0	25.0	0.037 ± 0.002	0.977	0.002
5.9	20	4	1:3	5.0	25.0	0.59 ± 0.03	0.984	0.551
5.10	40	8	1:3	5.0	25.0	0.61 ± 0.02	0.979	0.250
Influence of scavenger								
6.1	10	2	1:3	5.0	25.0	0.62 ± 0.009	0.995	0.052
6.2	10	2	1:3[b]	5.0	25.0	0.170 ± 0.009	0.975	0.142
6.3	10	2	1:3[c]	5.0	25.0	–	–	–
6.4	10	2	1:3[d]	5.0	25.0	0.031 ± 0.004	0.954	0.016
Influence of radiation								
7.1—UVC lamp	10	2	1:3	5.0	25.0	14.1 ± 0.2[e]	0.999	0.004
7.2—UVA lamp	10	2	1:3	5.0	25.0	5.88 ± 0.08[e]	0.998	0.009
7.3—Visible lamp	10	2	1:3	5.0	25.0	0.85 ± 0.07[e]	0.977	0.001
7.4—Suntest 300	10	2	1:3	5.0	25.0	4.0 ± 01[e]	0.993	0.040
7.5—Suntest 500	10	2	1:3	5.0	25.0	8.8 ± 0.5[e]	0.980	0.227
7.6—Solar	10	2	1:3	5.0		7.1 ± 0.2[e]	0.995	0.040
Real effluent								
8.1	36	8	1:3	5.0	25.0	0.89 ± 0.09	0.989	0.645

[a] Fe(III):citric acid molar ratio.
[b] Cr(VI):Oxalic acid molar ratio.
[c] Cr(VI):Maleic acid molar ratio.
[d] Cr(VI):EDTA molar ratio.
[e] k ($mg\,kJ_{UV}{}^{-1}$).

3.0, initially, the [Fe(Cit)] and the $[FeOH(Cit)]^-$ are the main photoactive species for all the Cr(VI):citric acid ratios tested (about 40 and 56%, respectively). At 1:1 Fe(III):citric acid molar ratio, although the same complexes are the main species at pH 3.0, the complexes $FeOH^{2+}$ and $Fe(OH)_2$ are also present in a significant amount in the solution (29.7 and 8.2%, respectively). As the reaction develops, the citric acid is consumed and the molar fraction of those Fe(III)-hydroxy complexes, with lower quantum yields for

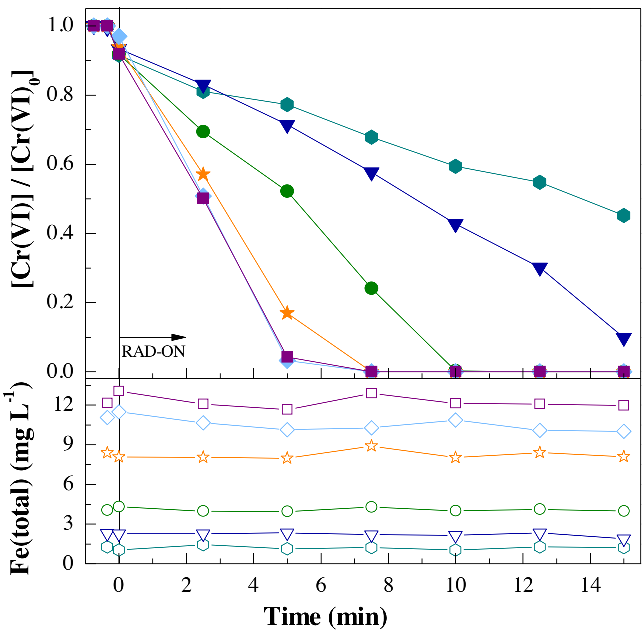

Fig. 2. Influence of iron concentration on Cr(VI) photocatalytic reduction ([Cr] = 10 mg L^{-1}) by Fe(III)/UVA–vis/citric acid system at pH 3 and 25c °C in the lab-scale photoreactor (SUNTEST at 500 W m^{-2}). Cr(VI)/citric acid molar ratio = 1:3, [Fe(III)] = (⬢, ⬡) 1 mg L^{-1}, (▼, ▽) 2 mg L^{-1}, (●, ○) 4 mg L^{-1}, (★, ☆) 8 mg L^{-1}, (◆, ◇) 10 mg L^{-1}, (■, □) 12 mg L^{-1}. Solid symbols—[Cr(VI)]/[Cr(VI)$_0$]; open symbols—[Fe(total)].

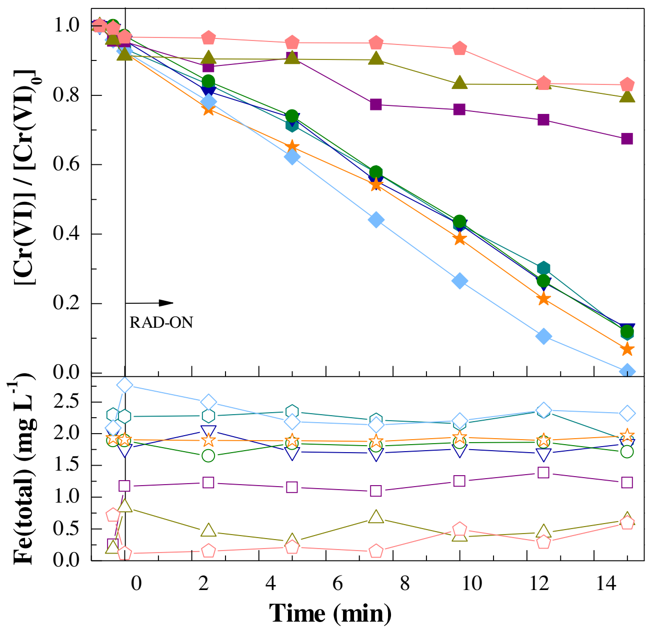

Fig. 3. Influence of pH value on Cr(VI) photocatalytic reduction ([Cr] = 10 mg L^{-1}) by Fe(III)/UVA–vis/citric acid system in the lab-scale photoreactor (SUNTEST at 500c W m^{-2}) with 2 mg L^{-1} of iron at 25 °C. Cr(VI)/citric acid molar ratio = 1:3, pH = (⬢, ⬡) 3.0, (▼, ▽) 3.5, (●, ○) 4.0, (★, ☆) 4.5, (◆, ◇) 5.0, (■, □) 6.0, (▲, △) 7.0, (⬟, ⬠) 8.0. Solid symbols—[Cr(VI)]/[Cr(VI)$_0$]; open symbols—[Fe(total)].

Fe(II) formation, increases. For higher Cr(VI):citric acid ratios, the [Fe(Cit)] and the $[FeOH(Cit)]^-$ are almost the only species present in the solution and the only factor that affects the reaction is the existence or not of the necessary citric acid amount.

3.2. Effect of iron concentration on the photocatalytic reduction of Cr(VI) by Fe(III)/UVA–vis/citric acid system

Since iron plays an important role in the Cr(VI) photoreduction reaction, its effect was evaluated in the lab-scale photoreactor (SUNTEST at 500 W m^{-2}) using initial Fe(III) concentrations of 1, 2, 4, 8, 10 and 12 mg L^{-1}, 10 mg L^{-1} Cr(VI), Cr(VI):citric acid molar ratio 1:3, pH 3.0 and 25 °C. The results are shown in Fig. 2 as a function of the reaction time and the zero-order kinetic constant values for each iron concentration are presented in Table 3.

It is possible to verify that the photocatalytic reduction rate of Cr(VI) increases with the Fe(III) concentration from 1 to 8 mg L^{-1}. With 1 mg L^{-1} of iron after 15 min of reaction only 50% of Cr(VI) was reduced. Nevertheless, with 2 mg L^{-1} of iron, after 15 min all the Cr(VI) was reduced to Cr(III). Doubling the iron dosage to 4 and then to 8 mg L^{-1}, the Cr(VI) total reduction time decreased to 10 and 7.5 min, respectively. However, for higher iron concentrations almost no improvement of reaction rate was observed. As reported by Soares et al. [32], higher iron concentrations require higher amounts of citric acid to be added in order to form the stable and strong complexes with ferric ions and to have, at the same time, the enough quantity to act as sacrificial agent of reactive oxygen species generated during the reaction, as above mentioned.

To determine the optimum iron amount for the reaction system it must be taken into account that iron is regenerated through a Fe(II)/Fe(III) photochemical cycle, that consists in: light absorption by Fe(III)-citrate complex, producing Fe(II) and radicals; oxidation of Fe(II) to Fe(III) by Cr(VI), accompanied by the intermediate production of Cr(IV) and Cr(V); reformation of Fe(III)-citrate complexes. In fact, it seems that it is not necessary to use a very high iron amount, only providing the sufficient amount for the photochemical cycle occurs. Therefore, the optimum iron dosage for the Cr(VI) reduction by the Fe(III)/UVA–vis/citric acid ternary system can be defined according to the discharge limits imposed by environmental authorities. Considering that the Portuguese legislation defines a discharge limit for total iron below 2 mg L^{-1} [2], this concentration was selected for further tests, thus avoiding any additional treatment costs associated with iron removal.

It must be also noted from Fig. 2 that the total dissolved iron remains constant during the entire reaction for all the concentrations studied. For Fe(III) dosages above 2 mg L^{-1}, on the other hand, the Fe(II) concentration remains near zero up to a point where it begins to increase, meaning that all the Cr(VI) was reduced (Fig. S6). The total chromium concentration remains also constant during all the reaction period, since the $Cr(OH)_3$ species only precipitates for pH values higher than 5.5.

3.3. Effect of pH on the photocatalytic reduction of Cr(VI) by Fe(III)/UVA–vis/citric acid system

The effect of solution pH on the Cr(VI) photoreduction kinetic rate by Fe(III)/UVA–vis/citric acid system was evaluated in the range of 3.0–8.0 with 10 mg L^{-1} of Cr(VI), Cr(VI):citric acid molar ratio of 1:3, 2 mg L^{-1} of iron and 25 °C in the lab-scale photoreactor (SUNTEST at 500 W m^{-2}). The results are shown in Fig. 3 and Table 3, where it is possible to observe that the pH plays a significant role in the Cr(VI) reduction. Increasing the pH value from 3.0 to 5.0, there is no evident difference between the photoreduction reaction rates, achieving the total Cr(VI) reduction in about 15 min. However, for pH values higher than 5.0, the Cr(VI) photoreduction reaction rates are very low and the total Cr(VI) reduction is not achieved.

Fig. S5(e) shows the molar fraction of each ferric citrate species under the conditions used in this study, calculated from the chemical equilibrium modelling system MINEQL+. At pH 3.0–6.0, [Fe(Cit)] and $[FeOH(Cit)]^-$ are the predominant species, being present in a total molar fraction higher than 95%. However, at pH 6.0, despite the high molar fraction of $[FeOH(Cit)]^-$ species (99.9%), only 33% of Cr(VI) was reduced (Fig. 3). This is probably due to the lesser

amount of protons present in the solution, not enough to reduce the Cr(VI) according to Eqs. (8) and (9).

$$HCrO_4^- + 7H^+ + 3e^- \leftrightarrow Cr^{3+} + 4H_2O \quad (8)$$

$$CrO_4^{2-} + 8H^+ + 3e^- \leftrightarrow Cr^{3+} + 4H_2O \quad (9)$$

Additionally, even controlling the pH during the reaction, fluctuations may occur and, for pH values higher than 6.0, the iron starts to precipitate as $Fe(OH)_{3(s)}$ (Fig. S5e), leading to a lower iron availability, decreasing, consequently, the Cr(VI) reduction rate. Nansheng et al. [33] reported also the important effect of the pH value on the photoreaction efficiency of a system containing Fe(III)-organic ligands complexes. On the other hand, the presence of citrate allowed the iron species stabilization through complexation with Fe(III), extending, this way, the reaction pH range [21]. Consequently, the observed Cr(VI) photoreduction rates between pH 3.0 and 5.0 had little differences. Beyond that, according to the solution pH values and Cr(VI) concentration used in this work, different hexavalent chromium species can be found in solution (Fig. S7). $HCrO_4^-$ is the dominant species at pH values between 3.0 and 5.0. For pH values higher than 5.0 the dominant species is CrO_4^{2-}, which requires more protons to achieve the total Cr(VI) reduction to Cr(III) (Eq. (8) and (9) for $HCrO_4^-$ and CrO_4^{2-} reductions, respectively). Taking this into account and to work at near legal discharge pH value (Decree-Law No. 238/98), the pH of 5.0 was selected as the optimum pH value.

It has to be noted that the total chromium concentration remained unchanged during the reaction period for pH values between 3.0 and 5.0. For higher pH values, the total chromium concentration had a small decrease mainly associated with the precipitation of trivalent chromium generated during the Cr(VI) reduction. As it is possible to observe from Fig. 3, the total dissolved iron concentration remained also constant for pH values between 3 and 5. However, at pH 6.0, a 50% reduction in iron content is observed due to its precipitation as $Fe(OH)_{3(s)}$ (Fig. S5 (e)). Moreover, for pH values equal or higher than 7.0, the total dissolved iron concentration in solution is near zero during all the reaction.

3.4. Effect of temperature on the photocatalytic reduction of Cr(VI) by Fe(III)/UVA–vis/citric acid system

The effect of solution temperature (15.0, 17.5, 20.0, 25.0, 30.0, 35.0 and 40.0 °C) on the reduction of 10 mg L^{-1} of Cr(VI) was assessed in the lab-scale photoreactor (SUNTEST at 500 W m^{-2}) at pH 5.0, 1:3Cr(VI):citric acid molar ratio and 2 mg L^{-1} of iron. Fig. 4 and Table 3 show that the kinetic rates of the experiments performed at 15.0 and 17.5 °C were particularly low, achieving total Cr(VI) reduction only after 35 min. Increasing the temperature to 20.0 °C, the Cr(VI) reduction rate was significantly improved and using higher temperatures (25.0, 30.0, 35.0 and 40.0 °C) a slightly faster Cr(VI) removal was even observed, with k values about 65% higher than the ones observed at the lower temperature values.

The Arrhenius equation (Eq. (10)) relates the reaction rate with temperature:

$$k = Ae^{-\frac{E_a}{RT}} \quad \text{or} \quad \ln k = \ln A - \frac{E_a}{R} \times \frac{1}{T} \quad (10)$$

where A, E_a, R, T and k are the frequency factor (mg L^{-1} min^{-1}), activation energy (J mol^{-1}), gas constant (8.314 J mol^{-1} K^{-1}), temperature (K) and kinetic constant (mg L^{-1} min^{-1}), respectively. The activation energy obtained for the reduction of Cr(VI) by Fe(III)/UVA–vis/citric acid system was 106 ± 3 kJ mol^{-1}. The activation energy value achieved was higher than the one obtained by Zhou et al. [34] (21.53 kJ mol^{-1}) for the Cr(VI) removal by nanoscale zero-valent iron (nZVI) coupled with ultrasound, suggesting that

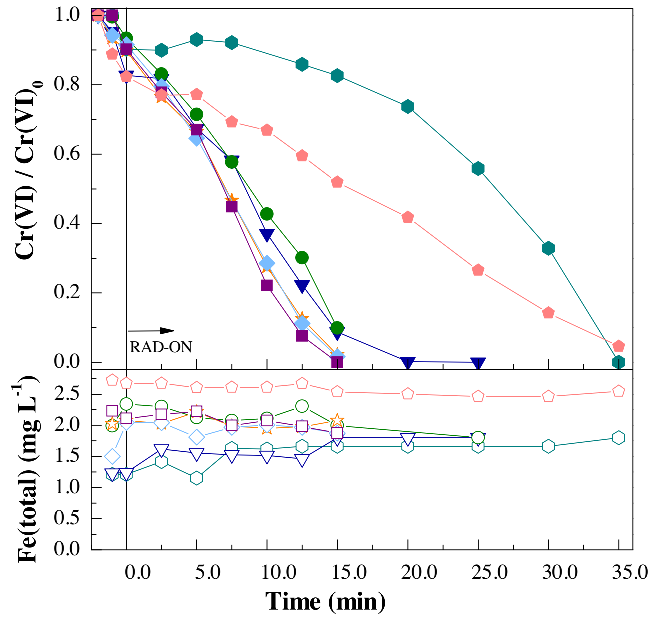

Fig. 4. Influence of temperature on Cr(VI) photocatalytic reduction ([Cr] = 10 mg L^{-1}) by Fe(III)/UVA-vis/citric acid system in the lab-scale photoreactor (SUNTEST at 500c W m^{-2}) with 2 mg L^{-1} of iron at pH 5.0. Cr(VI)/citric acid molar ratio = 1:3, temperature = (⬢, ⬡) 15 °C, (⬟, ⬠) 17.5 °C, (▼, ▽) 20.0 °C, (●, ○) 25 °C, (★, ☆) 30.0 °C, (◆, ◇) 35.5 °C, (■, □) 40.0 °C. Solid symbols—[Cr(VI)]/[Cr(VI)$_0$]; open symbols—[Fe(total)].

the ultrasound introduction probably enhances the chemical reaction.

According to the iron speciation diagrams at different temperatures calculated by the chemical equilibrium modelling system MINEQL+ (Figs. S8 and S5e), considering the concentrations of iron and citric acid used, $[FeOH(Cit)]^-$ molar fractions at pH 5.0 remained similar for all tested temperatures (around 99%). So, probably, the beneficial effect of high temperatures on the reaction rate is mainly associated with the enhancement of Fe^{2+} regeneration through the respective thermal reactions (Eqs. (11)–(13)) [21].

$$Fe^{3+} + H_2O_2 \rightarrow Fe^{2+} + HO^{\bullet}{}_2 + H^+ \quad (11)$$

$$Fe^{3+} + HO_2^{\bullet} \rightarrow Fe^{2+} + O_2 + H^+ \quad (12)$$

$$Fe^{3+} + O_2^{\bullet -} \rightarrow Fe^{2+} + O_2 \quad (13)$$

Despite the better results found at high temperatures, the solubility of ferric ions decreases. This could be perceived by the iron precipitation as $Fe(OH)_3$ at lower pH values when the temperature is increased. Figs. S8 and S5(e) shows that, despite the molar fraction of the photoactive species remained constant at pH 5.0, at 15 °C the iron starts to precipitate at pH 6.6 and at 40 °C it starts to precipitate at pH 5.7.

3.5. Effect of irradiation source on the photocatalytic reduction of Cr(VI) by Fe(III)/citric acid system

The photoreduction of photoactive Fe(III)-hydroxy and Fe(III)-citrate species changes according to the wavelength and intensity of the light source and solution pH. Beyond that, the solar light irradiance can vary during the day, according to seasons of the year, location and weather conditions. To clarify in detail the effect of light source wavelength and intensity on the photocatalytic reduction of 10 mg L^{-1} of Cr(VI) by Fe(III)-citrate complexes (1:3Cr(VI):citric acid molar ratio and 2 mg L^{-1} Fe(III)) at pH 5.0 and 25 °C, assays were performed using UVC, UVA and UVA-Vis lamps, simulated solar lights (300 and 500 W m^{-2}) and natural solar light.

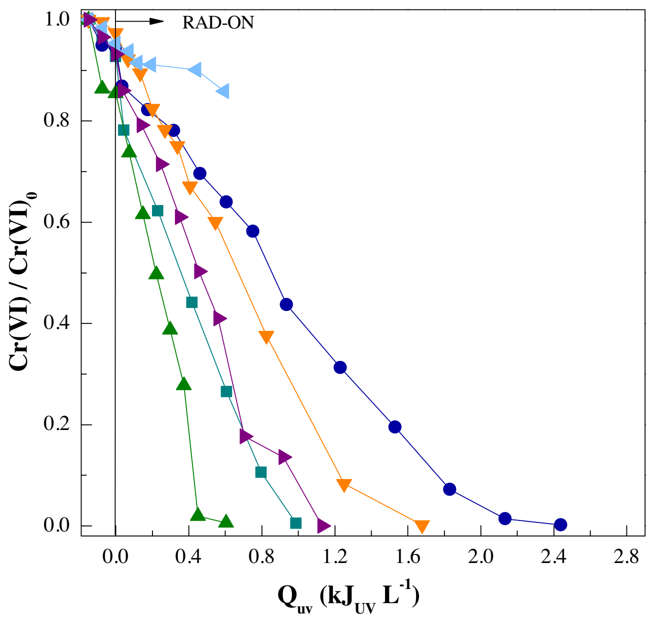

Fig. 5. Influence of irradiance source on Cr(VI) photocatalytic reduction ([Cr] = 10 mg L^{-1}) by Fe(III)/citric acid system with 2 mg L^{-1} of iron at pH 5.0 and 25 °C. Cr(VI)/citric acid molar ratio = 1:3; irradiance source = (■) SUNTEST at 500 W m^{-2}, (●) SUNTEST at 300 W m^{-2}, (▲) UVC lamp, (▼) UVA lamp, (◀) visible lamp, (▶) solar light; photonic fluxes determined by 2-NB actinometry (except for UVA–vis and UVC lamps).

Table 1 shows the different light sources, UV intensities and photonic fluxes.

Fig. 5 shows the photoreduction of Cr(VI) in Fe(III)-citrate solutions at pH 5.0 with different light irradiances as a function of accumulated energy calculated by Eqs. (5) and (6). The photonic fluxes were determined by the 2-NB actinometry method for UVA, simulated solar light (300 and 500 W m^{-2}) and natural solar light, by the ferrioxalate method for UVA–vis lamp and by the H_2O_2 method for UVC lamp. Cr(VI) reduction proved to be strongly dependent on the irradiance source. Using the UVA–vis lamp the Cr(VI) photoreduction was almost negligible. As reported in Table 1, this lamp has an average UV intensity, in the 280–400 nm wavelength range (0.3 W_{UV} m^{-2}), 10 times lower than the other light sources. Despite the UVA–vis lamp emits radiation in the 350–700 nm range, as reported by Moreira et al. [35], it exhibits large emission peaks at certain defined wavelengths: 436, 546 and 611 nm. This emphasizes that the use of mainly visible radiation leads to a lower Fe(III)-citrate complex photoreduction rate comparing with the use of UV. Low absorbance of Fe(III)-citrate complex in the visible range was already reported by Seraghini et al. [27], who observed higher absorbance near shorter wavelengths. In fact, the literature reports that UV and blue-light promote an efficient photolysis of Fe(III)-citrate complexes, with Fe(II) formation and oxidation of the ligand [36,37].

Fig. 5 shows that the results observed in this work are in accordance with the literature, since a significant enhancement of the Cr(VI) reduction was observed when the light source included the UV spectrum range. This way, the total Cr(VI) reduction (>99%) observed with the several UV lamps employed follows the order: SUNTEST at 300 W m^{-2} ($Q_{UV,n}$ = 2.44 kJ L^{-1}) < UVA lamp ($Q_{UV,n}$ = 1.68 kJ L^{-1}) < SUNTEST at 500 W m^{-2} ($Q_{UV,n}$ = 0.99 kJ L^{-1}) < UVC lamp ($Q_{UV,n}$ = 0.60 kJ L^{-1}). The SUNTEST lamp emits a continuous radiation in the range of 300–700 nm and the UVA lamp presents an emission wavelength peak at 360 nm; on the other hand, the UVC lamp emits mainly at 254 nm. The faster Cr(VI) reduction was achieved with UVC irradiance, probably because it exhibits higher photonic flux (0.72 J s^{-1}) than the other irradiation sources (SUNTEST 300 and 500 W m^{-2}: 0.34 and 0.44 J s^{-1}, respectively; UVA lamp: 0.65 J s^{-1}) and, as happens for the Fe(III)-hydroxy species, the quantum yield of Fe(III)-carboxylate species could be higher at lower wavelengths (<350 nm) [25]. Regarding the Cr(VI) reduction by the Fe(III)/UVA–vis/citric acid system with natural solar light in the CPC pilot plant, the total reduction was achieved with an accumulated energy of 1.13 kJ L^{-1}, a result very similar to the one obtained with SUNTEST at 500 W m^{-2}. Despite the experiment performed under natural solar light presented an average UV intensity similar to the one of the SUNTEST at 300 W m^{-2} (Table 1), the corresponding illuminated area/solution volume ratio (300 cm^2 L^{-1}) is higher than the one verified for the SUNTEST (170 cm^2 L^{-1}), probably leading to a higher efficiency. The results obtained with the photonic fluxes determined by the ferrioxalate actinometry method for all the irradiation sources (except for UVC lamp) are presented in Fig. S9 in the Supplementary material, and show very similar behaviors to the ones verified at Fig. 5.

It was decided to perform the next experiments in the lab-scale photoreactor (SUNTEST at 500 W m^{-2}) since it is the irradiation source more similar to the natural solar radiation at 12 a.m. on a sunny summer day in Northern Portugal (43.9 W_{UV} m^{-2}).

3.6. *Effect of initial Cr(VI) concentration on its photocatalytic reduction by Fe(III)/UVA–vis/citric acid system*

To examine the effect of the Cr(VI) initial concentration on its photoreduction rate, solutions with different Cr(VI) concentrations (1, 10, 20, 40 mg L^{-1}) were irradiated in the lab-scale photoreactor (SUNTEST at 500 W m^{-2}) using 0.576 mM of citric acid and 2 mg L^{-1} of Fe(III), at pH 5.0 and 25 °C. These iron and citric acid concentrations were optimized in the previous sections for the reduction of 10 mg L^{-1} of Cr(VI). As it is possible to observe in Fig. 6a, contrary to results reported by Liu et al. [14] regarding the photocatalytic reduction of Cr(VI) by a Fe(III)/bisphenol A system, the photoreduction rate decreased with increasing Cr(VI) initial concentrations (Table 3, experiments 5.1–5.4). For the lower concentration (1 mg L^{-1}), the total Cr(VI) reduction was achieved after 5 min of reaction. With 10 mg L^{-1} of Cr(VI) (the dosage studied in the previous points), the Cr(VI) total reduction was achieved after 15 min of reaction.

However, increasing the Cr(VI) initial concentration to values of 20 and 40 mg L^{-1}, the Cr(VI) total reduction is not reached. After 90 min of reaction, the Cr(VI) in solution remains almost constant (Fig. 6a). As it was above concluded, there is an adequate Cr(VI):citric acid molar ratio, which was found to be 1:3. So, when the Cr(VI) initial concentration was increased to 20 and 40 mg L^{-1}, the Cr(VI) reduction stopped when all the citric acid present in solution was consumed, not existing enough amount to act both as scavenger agent of reactive oxygen species generated from the photoreduction of Fe(III)-citrate complexes and to form strong complexes with the ferric ions. This way, new experiments were performed increasing the citric acid dosage as the Cr(VI) initial concentration increases, maintaining the ratio 1:3. The iron concentration was kept at 2 mg L^{-1}, since, in principle, iron is regenerated through the Fe(II)/Fe(III) photochemical cycle while the Cr(VI) is reduced to Cr(III). However, as it is possible to observe in Fig. 6b, the total reduction of 20 mg L^{-1} of Cr(VI) was achieved after 60 min, but when the initial Cr(VI) concentration is increased to 40 mg L^{-1}, the total Cr(VI) reduction was not achieved at the end of the reaction time (90 min), even increasing the citric acid concentration. This can be attributed to the fact that with a higher chromium concentration and with the same iron dosage for the Fe(II)/Fe(III) photochemical cycle more time is required to achieve the total Cr(VI) reduction. To increase the reaction rate,

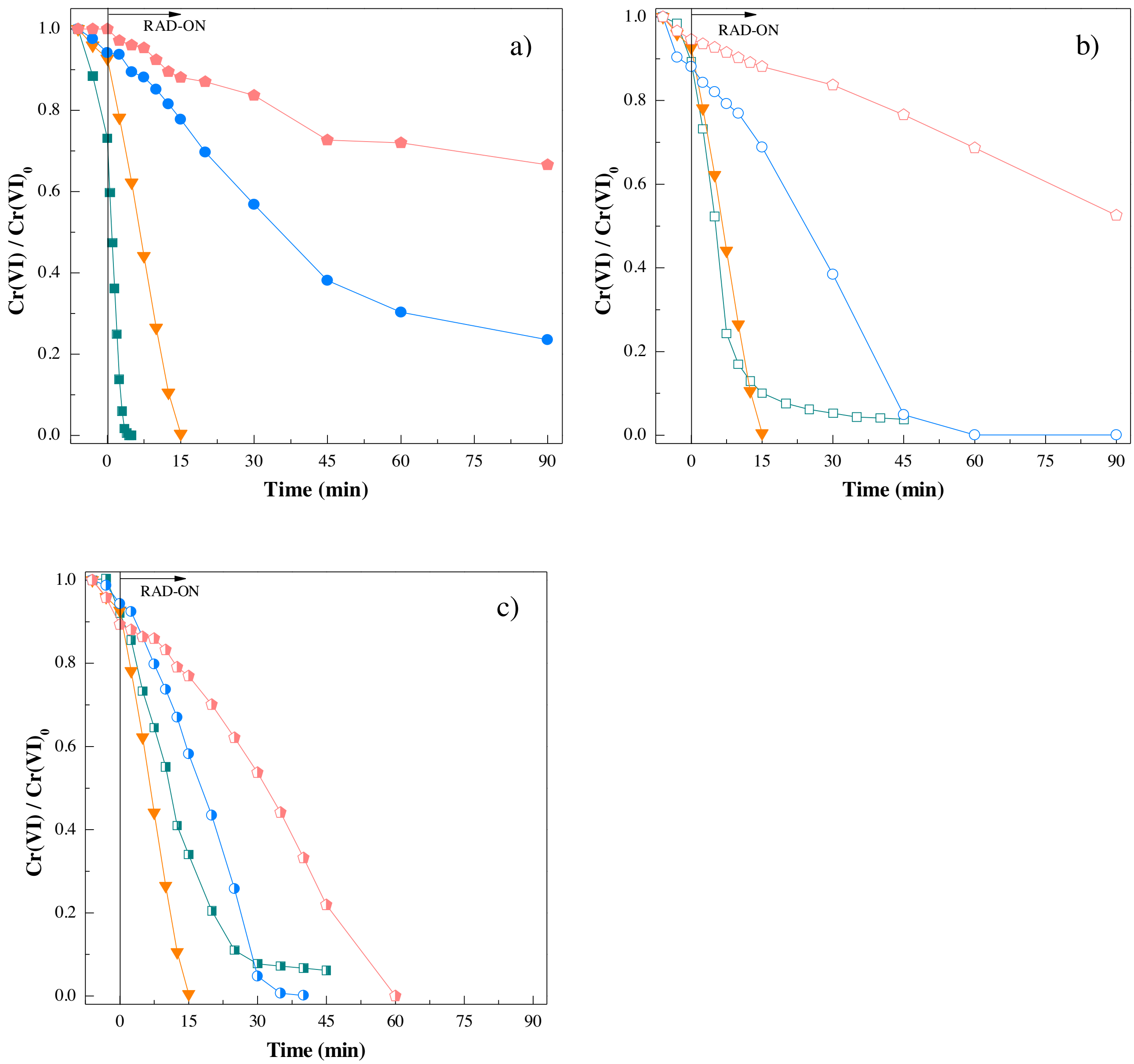

Fig. 6. Influence of Cr(VI) initial concentration on its photocatalytic reduction by Fe(III)/UVA-vis/citric acid system at pH 5.0 and 25 °C in the lab-scale photoreactor (SUNTEST at 500 W m^{-2}), with the respective Cr(VI) initial concentration and Cr(VI):citric acid:[Fe(III)] molar ratio: a) (■) [Cr(VI)] = 1 mg L^{-1} and 1:30:2; (▼) [Cr(VI)] = 10 mg L^{-1} and 1:3:2; (●) [Cr(VI)] = 20 mg L^{-1} and 1:1.5:2; (⬟) [Cr(VI)] = 40 mg L^{-1} and 1:0.75:2. b) (□) [Cr(VI)] = 1 mg L^{-1} and 1:3:2; (▼) [Cr(VI)] = 10 mg L^{-1} and 1:3:2; (○) [Cr(VI)] = 20 mg L^{-1} and 1:3:2; (⬠) [Cr(VI)] = 40 mg L^{-1} and 1:3:2. **c)** (◧) [Cr(VI)] = 1 mg L^{-1} and 1:3:0.2; (▼) [Cr(VI)] = 10 mg L^{-1} and 1:3:2; (◐) [Cr(VI)] = 20 mg L^{-1} and 1:3:4; (⬟) [Cr(VI)] = 40 mg L^{-1} and 1:3:8.

probably it is necessary to increase also the iron dosage. Consequently, new tests were performed doubling Cr(VI) and citric acid concentrations, when the iron dosage also doubled. These results are represented in Fig. 6c, where it is possible to check that the total Cr(VI) removal is now achieved in all cases within the pre-defined reaction time and more quickly than in the previous conditions. These results are corroborated by the higher photodegradation rate constants attained in the latter experiments, as can be seen from Table 3. In conclusion, to achieve a total Cr(VI) reduction, the molar ratio 1:3 between the Cr(VI) and the citric acid must be maintained, as well as the iron concentration should be increased/decreased in the same proportion.

It must also be noted that even in the optimized experimental conditions, a higher Cr(VI) concentration takes more time to be reduced than a lower one. This could be explained by the chromium speciation diagrams at different concentrations (Fig. S10 of Supplementary material), where it is possible to see that, at pH 5.0, increasing the Cr(VI) initial concentration, the molar fraction of the $HCrO_4^-$ species decreases (97.3, 96%, 95% and 93% for 1, 10, 20 and 40 mg L^{-1}, respectively) with the appearance of the CrO_4^{2-} species, that requires more protons to be reduced (Eqs. (8) and (9). For all conditions tested, the photoactive complex $[FeOH(Cit)]^-$ was the main species at pH 5.0 (Fig. S11).

3.7. Effect of Fe(III)-carboxylate complex on the photocatalytic reduction of Cr(VI)

The addition of scavenging agents to generate stable ferric complexes appears as an alternative to prevent iron precipitation in the Fenton reaction and to increase the reaction rate, through the generation of Fe(II) with improved quantum yield from the Fe(III)-carboxylate complexes over Fe(III)-hydroxy complexes, due

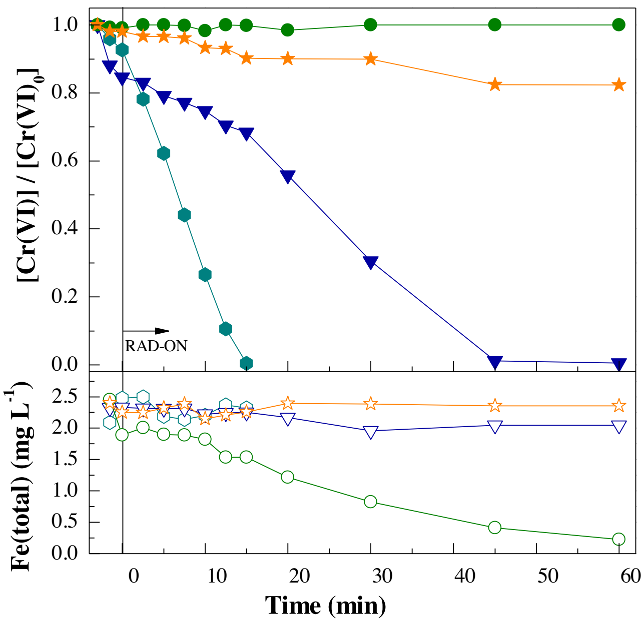

Fig. 7. Influence of scavenging agent on Cr(VI) photocatalytic reduction ([Cr] = 10 mg L^{-1}) by Fe(III)/scavenging agent system with Cr(VI)/scavenging agent molar ratio of 1:3, 2 mg L^{-1} of iron at pH 5.0 and 25 °C in the lab-scale photoreactor (SUNTEST at 500 W m^{-2}). Scavenging agent = (⬢, ⬡) citric acid, (▼, ▽) oxalic acid, (●, ○) maleic acid, (★, ☆) EDTA. Solid symbols—[Cr(VI)]/[Cr(VI)$_0$]; open symbols—[Fe(total)].

to the higher absorption of UV–vis light. This way, these ferricarboxylate complexes allow the use of a higher fraction of the solar radiation spectrum and are more soluble than ferric iron-water complexes, allowing also to work at neutral pH values, without iron precipitation [38]. Different studies report the use of ferric complexes in modified photo-Fenton processes through the addition of oxalic acid [39], citric acid [40] and ethylenediaminetetraacetic acid (EDTA) [41]. In this work, different Fe(III)-carboxylate complexes were tested on the photocatalytic reduction of 10 mg L^{-1} of Cr(VI) with 2 mg L^{-1} of Fe(III) at pH 5.0 and 25 °C in the lab-scale photoreactor (SUNTEST at 500 W m^{-2}) through the addition of citric acid, oxalic acid, maleic acid and EDTA at Cr(VI)/scavenging agent molar ratios of 1:3 (optimal ratio for citric acid found in this study). In these circumstances the Fe(III)/scavenging agent molar ratio is 1:16 for citrate acid, oxalic acid, maleic acid and EDTA. The citrate and oxalate are present in carbon-rich surface waters, atmospheric water, and drainage water from forested and agricultural watersheds. Moreover, oxalate was found to be able to enhance the ferric-catalyzed photoreduction of Cr(VI) [42].

Fig. 7 shows that the scavenging agent performance for the Cr(VI) reduction increases in the following order: maleic acid < EDTA < oxalic acid < citric acid. The greater efficiency observed with citric and oxalic acids may be explained by the presence of carboxylic groups in their structures which are able to form photoactive complexes with Fe(III) under the conditions used in this study. During the solar photolysis of these complexes, Fe(II) ions and reactive oxygen species are generated. As a result, Cr(VI) is reduced to Cr(III) by Fe(II). Despite the addition of oxalic acid contributed also to a good efficiency, during the reaction its consumption probably leads to insufficient oxalate amounts to form the complex again, decreasing, consequently, the quantum yield for ferrous production. On the other hand, citric acid proved to be more efficient, since it is present in solution in enough quantity to form the Fe(III)-citrate complexes during the entire reaction and, more importantly, it is known that the respective quantum yield, at the pH conditions under study (5.0), is higher than the one of the oxalate. In fact, Abrahamson et al. [36] reported that increasing the pH value from 2.7 to 4.0 the citric acid quantum yield increased about 50%, while for oxalate decreases by 50%.

Rivero-Huguet and Marshall [43] reported a Cr(VI) reduction of about 55% in 1800 min in the presence of zero-valent iron (ZVI) and EDTA, at the same conditions used in this work. Similarly, a bad performance of Fe(III)/UVA–vis/EDTA system for Cr(VI) photoreduction was achieved in the present study. The scavenging agents used in this work can be classified into two groups according to the formation or not of photocatalytic active ferricarboxylate complexes. Only scavenging agents forming active ferricarboxylate complexes are able to improve the photocatalytic reduction rate of Cr(VI) since their photolysis yields Fe(II) and low oxidizing species, avoiding the reoxidation of chromium species. As was also observed by Rodríguez et al. [25], maleic acid does not produce ferricarboxylate complexes under the studied experimental conditions and, as a consequence, its presence does not improve Cr(VI) reduction rate. Thus, after 15 min of reaction, Cr(VI) photoreduction increases from 0.19 and 9.8% in the absence of photoactive carboxylate complexes (with EDTA and maleic acid, respectively) up to 31.6 and 99.6% in the presence of photoactive oxalate and citrate complexes, respectively. To clarify in detail the type of Fe(III)-carboxylate species acting in each system, Fe(III) speciation diagrams were calculated with each scavenging agent used in this study as a function of the solution pH considering the initial experimental conditions. From Figs. S5(e) and S12 it is possible to confirm the formation of photoactive species $[FeOH(Cit)]^-$ and $[Fe(Ox)_3]^{3-}$ at pH 5.0 in the presence of citric and oxalic acid, respectively. In spite of both Fe(III)-carboxylate species are present in high molar fractions (99.3% of [FeOH(Cit)] and 94.5% of $[Fe(Ox)_3]^{3-}$), the best results were achieved with Fe(III)-citrate complexes since they have higher quantum yield, at the conditions of this study, as abovementioned. In the case of EDTA addition, although it appears to form also a high molar fraction of [Fe(EDTA)] complex (99.8%) at pH 5.0, this complex should not be photoactive in the conditions of this work, since almost no Cr(VI) reduction was attained during 1 h of reaction. The speciation diagram of Fe(III) with maleic acid addition proved that this organic ligand does not produce ferricarboxylate complexes at pH 5.0 (Fig. S12b). At this pH value, the iron is all precipitated as $Fe(OH)_3$.

Despite having been reported by Lee et al. [44] that the Cr(VI) photocatalytic reduction by a TiO_2 suspension was strongly affected by the number of carboxylic groups in the organic compounds added, in this work, Fe(III) photocatalytic reduction of Cr(VI) in the presence of organic compounds does not exhibit a linear correlation with the number of carboxylic groups of the scavenging agent. Sun et al. [28] reported similar results and suggested that the key factor to achieve good efficiencies with this type of systems is the presence of α-OH groups in the organic molecule. Kabir-ud-Din et al. [45] described the formation of a ring structure between Mn(II) and an organic acid, which improved the α-OH group activity, resulting in the formation of a Cr(VI)-organic acid-Mn(II) complex. However, in this study, only the citric acid presents one α-OH group, and, despite not having α-OH groups, oxalic acid proved also to enhance the Cr(VI) photocatalytic reduction. Therefore, it is believed that to achieve a good process efficiency, there must be a compromise between the photoactive species formation among iron and the scavenging agent and the number of α −OH groups, as well as with the respective quantum yield.

Beyond the influence of quantum yields for Fe(II) formation on the Cr(VI) reduction efficiency, the rate of Fe(III)-carboxylate complexes photodecarboxylation can also affect the process since their presence allows preserving dissolved iron in solution with the consequent enhancement of Cr(VI) removal. It has to be noted that for all tested organic ligands, the total dissolved iron concentration remained almost constant during the entire reaction period, with

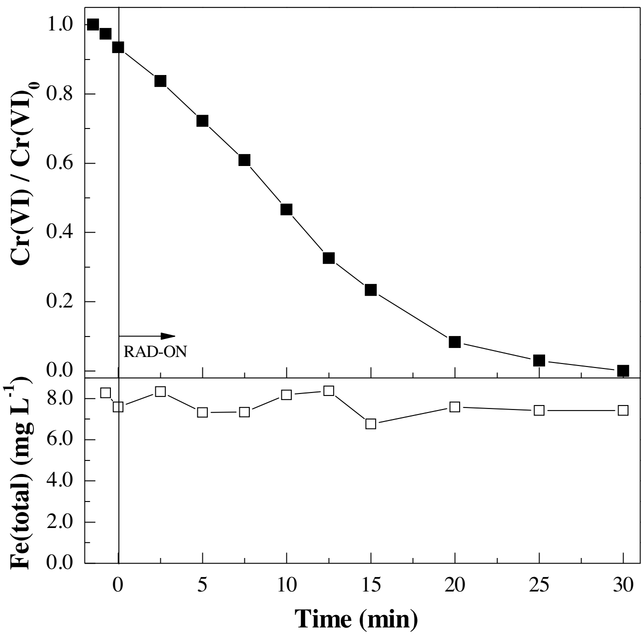

Fig. 8. Photoreduction of Cr(VI) present in a real wastewater sample by a Fe(III)/UVA-vis/citric acid system with 1:3Cr(VI):citric acid molar ratio and 8 mg L^{-1} of iron at pH 5.0, 25 °C in the lab-scale photoreactor (SUNTEST at 500 W m^{-2}). Solid symbol—[Cr(VI)]/[$Cr(VI)_0$]; open symbol—[Fe(total)].

exception for maleic acid case, where it is possible to observe that, as abovementioned, the iron precipitates (Fig. 7).

3.8. Real wastewater containing Cr(VI)

Table 2 presents the main characteristics of a Cr(VI) containing wastewater sample from a galvanic industry of northern Portugal. The Cr(VI) concentration (36 mg L^{-1}) is well above the allowed limit (0.1 mg L^{-1}) for discharge into receiving water bodies as established by the Portuguese legislation (Decree-Law No. 236/98 [2]). The photoreduction of Cr(VI) present in this wastewater was conducted using the previously optimized conditions: 1:3 Cr(VI):citric acid molar ratio, 8 mg L^{-1} of iron, pH 5.0 and 25 °C in the lab-scale photoreactor (SUNTEST at 500 W m^{-2}). The total reduction of Cr(VI) was achieved in 30 min (Fig. 8), proving the efficiency of the optimized Fe(III)/UVA-vis/citric acid system for the treatment of Cr(VI) containing wastewaters. Other authors achieved similar results but at acidic pH values. Lugo-Lugo et al. [46] studied the Cr(VI) reduction present in chromium electroplating wastewater with a bimetallic (Cu/Fe) galvanic reactor achieving 100% of chromium reduction in about 25 min for a pH value of 2.0 and a ratio of copper to iron surface areas of 3.5:1. In this case, despite the total dissolved iron concentration remained constant during all the reaction (Fig. 8), it was observed that the iron(II) starts to be in excess before all the Cr(VI) is reduced to Cr(III) (Fig. S13) since it was added in a higher initial concentration to keep the optimized Fe(III)/UVA–vis/citric acid ratio.

4. Conclusions

Solar photocatalytic reduction of hexavalent chromium was successfully achieved using a Fe(III)/UVA–vis system in the presence of citric acid. The reaction kinetics depends on the citric acid amount present in the solution: the maximum rate was attained for a Cr(VI):citric acid molar ratio equal to 1:3, using 2 mg L^{-1} of Fe(III) (total iron emission limit for the discharge of treated effluents according to the Portuguese legislation) for an initial Cr(VI) concentration of 10 mg L^{-1}. The presence of citrate allowed to extend the pH range of the reaction through complexation with Fe(III), allowing to work at near neutral pH values (5.0, the optimum pH value found). In turn, the increase of the solution temperature improved significantly the reaction rate in the range under study (15.0–40.0 °C). Among the artificial sources of light, the Cr(VI) reduction was more effective using UVC and UVA–vis (SUNTEST at 500 W m^{-2}) irradiances, attaining the complete reduction after 0.60 and 0.99 kJ L^{-1}, respectively. The use of natural solar light in the CPC pilot plant led to results very similar to the Cr(VI) reduction in the SUNTEST at 500 W m^{-2}. It was also concluded that the Fe(III) concentration should be adjusted in proportion to the Cr(VI) initial concentration. The rate constants involving the four organic ligands tested were in the order: citric acid > oxalic acid > EDTA > maleic acid, suggesting that it must exist a compromise between the fraction of photoactive species formed and the number of α-OH of each organic molecule, as well as with the respective quantum yield. This work discards the reported idea that the Cr(VI) reduction kinetics depends on the number of carboxylic groups or on the number of α-OH of the organic acids.

To close, this system proved to be very promising in the treatment of real Cr(VI) containing wastewaters from galvanization processes, showing also that it could be useful for the simultaneous removal of some organic pollutants present in the natural aqueous environment.

Acknowledgments

This work was co-financed by FCT and FEDER under Programme PT2020 (Project UID/EQU/50020/2013–POCI-01-0145-FEDER-006984) and by QREN, ON2 and FEDER (Projects NORTE-07-0162-FEDER-000050 and NORTE-07-0124-FEDER-000008). V.J.P. Vilar acknowledges the FCT Investigator 2013 Programme (IF/01501/2013). B.A. Marinho acknowledges Capes for her scholarship (BEX-0983-13-6). R.O. Cristóvão thanks FCT for her Post-doc Scholarship (SFRH/BPD/81564/2011).

Appendix A. Supplementary data

Supplementary data associated with this article can be found, in the online version, at http://dx.doi.org/10.1016/j.apcatb.2016.03.061.

References

[1] M.I. Litter, Appl. Catal. B: Environ. 23 (1999) 89–114.
[2] M.d. Ambiente, Decreto-Lei n.o 236/98, 176, Diário Da República—I Série-A, 1998, pp. 3676–3722.
[3] U.S. EPA, IRIS Toxicological Review of Hexavalent Chromium (2010 External Review Draft), in: U.S.E.P. Agency (Ed.), EPA/635/R-10/004A, Washington, DC, 2010.
[4] X. Lv, Y. Hu, J. Tang, T. Sheng, G. Jiang, X. Xu, Chem. Eng. J. 218 (2013) 55–64.
[5] F. Depault, M. Cojocaru, F. Fortin, S. Chakrabarti, N. Lemieux, Toxicol. In Vitro 20 (2006) 513–518.
[6] D. Petruzzelli, R. Passino, G. Tiravanti, Ind. Eng. Chem. Res. 34 (1995) 2612–2617.
[7] S.E. Bailey, T.J. Olin, R.M. Bricka, D.D. Adrian, Water Res. 33 (1999) 2469–2479.
[8] P. Lakshmipathiraj, G. Bhaskar Raju, M. Raviatul Basariya, S. Parvathy, S. Prabhakar, Sep. Purif. Technol. 60 (2008) 96–102.
[9] A. Hafiane, D. Lemordant, M. Dhahbi, Desalination 130 (2000) 305–312.
[10] C.D. Palmer, P.R. Wittbrodt, Environ. Health Perspect. 92 (1991) 25–40.
[11] CL:AIRE, Treatment of Chromium Contamination and Chromium Ore Processing Residue, Technical Bulletin (TB 14). Contaminated Land: Applications in Real Environment, London, UK, 2007.
[12] M.A. Hashim, S. Mukhopadhyay, J.N. Sahu, B. Sengupta, J. Environ. Manag. 92 (2011) 2355–2388.
[13] D. Nansheng, W. Feng, L. Fan, X. Mei, Chemosphere 36 (1998) 3101–3112.
[14] Y. Liu, L. Deng, Y. Chen, F. Wu, N. Deng, J. Hazard. Mater. 139 (2007) 399–402.
[15] OECD, OECD guidelines for the testing of chemicals, in: Test N°. 302B: Inherent Biodegradability: Zahn–Wellens/EMPA, OECD Publishing, 1992.
[16] H.J. Kuhn, S.E. Braslavsky, R. Schmidt, Chemical actinometry (IUPAC technical report), Pure Appl. Chem. (2004) 2105.

[17] K.L. Willett, R.A. Hites, J. Chem. Educ. 77 (2000) 900.
[18] I. Nicole, J. De Laat, M. Dore, J. Duguet, C. Bonnel, Water Res. 24 (1990) 157–168.
[19] P. Soares, T.C.V. Silva, D. Manenti, S.A.G.U. Souza, R.R. Boaventura, V.P. Vilar, Environ. Sci. Pollut. Res. 21 (2014) 932–945.
[20] J.H.O.S. Pereira, V.J.P. Vilar, M.T. Borges, O. González, S. Esplugas, R.A.R. Boaventura, Sol. Energy 85 (2011) 2732–2740.
[21] F.C. Moreira, R.A.R. Boaventura, E. Brillas, V.J.P. Vilar, Appl. Catal. B: Environ. 162 (2015) 34–44.
[22] P. Mytych, Z. Stasicka, Appl. Catal. B: Environ. 52 (2004) 167–172.
[23] P.R. Wittbrodt, C.D. Palmer, Environ. Sci. Technol. 29 (1995) 255–263.
[24] C. Li, Y.-Q. Lan, B.-L. Deng, Pedosphere 17 (2007) 318–323.
[25] E.M. Rodríguez, B. Núñez, G. Fernández, F.J. Beltrán, Appl. Catal. B: Environ. 89 (2009) 214–222.
[26] Y. Chen, Z. Liu, Z. Wang, M. Xue, X. Zhu, T. Tao, J. Hazard. Mater. 194 (2011) 202–208.
[27] N. Seraghni, S. Belattar, Y. Mameri, N. Debbache, T. Sehili, Int. J. Photoenergy (2012) 10.
[28] J. Sun, J.D. Mao, H. Gong, Y. Lan, J. Hazard. Mater. 168 (2009) 1569–1574.
[29] G. Colón, M.C. Hidalgo, J.A. Navío, Langmuir 17 (2001) 7174–7177.
[30] J.M. Meichtry, M. Brusa, G. Mailhot, M.A. Grela, M.I. Litter, Appl. Catal. B: Environ. 71 (2007) 101–107.
[31] A.M.N. Silva, X. Kong, M.C. Parkin, R. Cammack, R.C. Hider, Dalton Trans. (2009) 8616–8625.
[32] P.A. Soares, M. Batalha, S.M.A.G.U. Souza, R.A.R. Boaventura, V.J.P. Vilar, J. Environ. Manag. 152 (2015) 120–131.
[33] D. Nansheng, W. Feng, L. Fan, L. Zan, Chemosphere 35 (1997) 2697–2706.
[34] X. Zhou, B. Lv, Z. Zhou, W. Li, G. Jing, Chem. Eng. J. 281 (2015) 155–163.
[35] F.C. Moreira, J. Soler, A. Fonseca, I. Saraiva, R.A.R. Boaventura, E. Brillas, V.J.P. Vilar, Appl. Catal. B: Environ. 182 (2016) 161–171.
[36] H.B. Abrahamson, A.B. Rezvani, J.G. Brushmiller, Inorg. Chim. Acta 226 (1994) 117–127.
[37] W. Feng, D. Nansheng, Chemosphere 41 (2000) 1137–1147.
[38] D. Prato-Garcia, R. Vasquez-Medrano, M. Hernandez-Esparza, Sol. Energy 83 (2009) 306–315.
[39] A.V. Schenone, L.O. Conte, M.A. Botta, O.M. Alfano, J. Environ. Manag. 155 (2015) 177–183.
[40] C. Ruales-Lonfat, J.F. Barona, A. Sienkiewicz, J. Vélez, L.N. Benítez, C. Pulgarín, Appl. Catal. B: Environ. 180 (2016) 379–390.
[41] M. Engelmann, R. Bobier, T. Hiatt, I.F. Cheng, Biometals 16 (2003) 519–527.
[42] S.J. Hug, H.-U. Laubscher, B.R. James, Environ. Sci. Technol. 31 (1997) 160–170.
[43] M. Rivero-Huguet, W.D. Marshall, Chemosphere 76 (2009) 1240–1248.
[44] S.M. Lee, I.H. Cho, Y.Y. Chang, J.K. Yang, J. Environ. Sci. Health 42 (2007) 543–548.
[45] D. Kabir ud, K. Hartani, Z. Khan, Transit. Met. Chem. 25 (2000) 478–484.
[46] V. Lugo-Lugo, C. Barrera-Díaz, B. Bilyeu, P. Balderas-Hernández, F. Ureña-Nuñez, V. Sánchez-Mendieta, J. Hazard. Mater. 176 (2010) 418–425.